

Article

Additive manufacturing of a point-of-care “polypill”: Fabrication of concept capsules of complex geometry with bespoke release against cardiovascular disease

Pereira, Beatriz, Isreb, Abdullah, Isreb, Mohammad, Forbes, Robert Thomas, Oga, Enoche Florence and Alhnan, Mohamed

Available at <http://clock.uclan.ac.uk/33324/>

Pereira, Beatriz, Isreb, Abdullah, Isreb, Mohammad, Forbes, Robert Thomas ORCID: 0000-0003-3521-4386, Oga, Enoche Florence ORCID: 0000-0002-2661-0574 and Alhnan, Mohamed (2020) Additive manufacturing of a point-of-care “polypill”: Fabrication of concept capsules of complex geometry with bespoke release against cardiovascular disease. Advanced Healthcare Materials, 9 (13). ISSN 2192-2640

It is advisable to refer to the publisher’s version if you intend to cite from the work.
<http://dx.doi.org/10.1002/adhm.202000236>

For more information about UCLan’s research in this area go to <http://www.uclan.ac.uk/researchgroups/> and search for <name of research Group>.

For information about Research generally at UCLan please go to <http://www.uclan.ac.uk/research/>

All outputs in CLoK are protected by Intellectual Property Rights law, including Copyright law. Copyright, IPR and Moral Rights for the works on this site are retained by the individual authors and/or other copyright owners. Terms and conditions for use of this material are defined in the [policies](#) page.

1

2 Additive manufacturing of a point-of-care
3 “polypill”: Fabrication of concept capsules of
4 complex geometry with bespoke release against
5 cardiovascular disease

6

7 *Beatriz C. Pereira, Abdullah Isreb, Mohammad Isreb, Robert T. Forbes, Enoche F. Oga**,
8 *Mohamed A. Alhnan***

9

10

11 B. C. Pereira, Dr. A. Isreb, Prof. R. T. Forbes, *Dr. E. F. Oga,

12 School of Pharmacy & Biomedical Sciences

13 University of Central Lancashire

14 Fylde road, PR1 2HE, UK

15 E-mail: EOga@uclan.ac.uk

16

17 **Dr M. A. Alhnan

18 Institute of Pharmaceutical Sciences

19 King’s College London

20 5.77 Franklin Wilkins Building, 150 Stamford Street, SE1 9NH, UK

21 E-mail: alhnan@kcl.ac.uk

22

23 Keywords: multidrug, fixed dose combination (FDC), digital health, computer-aided design
24 (CAD), controlled-release, in vitro-in vivo correlation

25

26 **Abstract**

27 Polypharmacy is often needed for the management of cardiovascular diseases and
28 is associated with poor adherence to treatment. Hence, highly flexible and adaptable
29 systems are in high demand to accommodate complex therapeutic regimens. A novel
30 design approach was employed to fabricate highly modular 3D printed 'polypill'
31 capsules with bespoke release patterns for multiple drugs. Complex structures were
32 devised using combined fused deposition modelling 3D printing aligned with hot-
33 filling syringes. Two unibody highly modular capsule skeletons with 4 separate
34 compartments were devised: i) concentric format: two external compartments for
35 early release whilst two inner compartments for delayed release, or ii) parallel
36 format: where non-dissolving capsule shells with free-pass corridors and dissolution
37 rate-limiting pores were used to achieve immediate and extended drug releases,
38 respectively. Controlling drug release was achieved through digital manipulation of
39 shell thickness in the concentric format or the size of the rate limiting pores in the
40 parallel format. Target drug release profiles were achieved with variable orders and
41 configurations, hence confirming the modular nature with capacity to accommodate
42 therapeutics of different properties. Projection of the pharmacokinetic profile of this
43 digital system capsules revealed how the developed approach could be applied in
44 dose individualization and achieving multiple desired pharmacokinetic profiles.

45

46 **1. Introduction**

47 Population-based surveys and cross-sectional studies have shown that polypharmacy affects 40-
48 50% of elderly patients in high income countries.^[1-3] Among chronic conditions, cardiovascular
49 disease (CVD) accounts for 45% of all deaths in Europe^[4] and its management necessitates a
50 complex therapeutic regimen, which usually includes anti-platelet, anti-hypertensive and lipid-
51 lowering agents.^[5] Such complex treatment has been linked to many issues, including
52 psychological distress, depressing symptoms and poor adherence among patients.^[6-8] Common
53 strategies to improve patient compliance include the use of medication boxes or technologies like
54 PillPack dispensing system, alarms to remember dose times, medicines administration records
55 (MARS), and smartphone applications such as My Medication Passport.^[9-11]

56 However, these approaches are usually associated with instructions that may be hard-to-read,
57 understand and/or even follow by elderly patients.^[12] Additionally, daily medication boxes often
58 contain different unlabelled tablets/capsules that may have similar physical appearance and might
59 lead to dispensing, patients or carers errors. Therefore, technology-based approaches need a more
60 rigorous evaluation of cost-effectiveness and patient acceptability, suggesting that a more
61 simplified and efficient strategy is needed.^[13] Polypills can simplify the dosing regimen without
62 compromising the therapeutic plan. The rapidly growing interest in this approach resulted in the
63 progression of several combinations of drugs to clinical trials and registered products.^[14] Despite
64 their proven advantages, the rigid nature of fixed multiple-drug combination in a single pill may
65 be suitable for a limited number of patients. Hence, a highly adaptable manufacturing technique
66 that allows easy selection and titration of multiple drug doses is needed.

67 3D printing is an emerging production method with potential superior agility in the production of
68 on-demand medicines, with a small number of processing steps, low costs and flexibility of
69 design.^[15, 16] Several studies have reported the applicability of fused deposition modelling (FDM)
70 3D printing in the production of solid dosage forms.^[17-19] Its advantage of medicine
71 personalization has been extensively explored, in special patient groups (e.g. paediatrics), by

72 improving characteristics such as palatability,^[20] and by fabrication of a ‘dynamic dose combiner’
73 which can be easily shaped to each patient’s needs.^[21, 22]

74 To optimise therapeutic effect, controlling drug release from 3D printing technologies was
75 achieved by modifying printing parameters e.g. infill percentage,^[23, 24] or the shape or size of the
76 dosage form.^[25] 3D printed capsules avoid the high temperatures usually required with FDM 3D
77 printing. An early attempt of FDM 3D printing of a pulsatile release capsule system was reported
78 in 2015.^[26] Further studies have achieved delayed^[27, 28] or pulsatile release capsules.^[29] The
79 capsules were manufactured in two pieces to be manually assembled in a second step. Therefore,
80 a one-step ‘print and fill’ capsule was developed.^[30, 31] However, the use of water-based
81 formulations was linked to moisture absorption by Polyvinyl(alcohol) (PVA) shells with swelling,
82 wall delamination and leakage of the infill. Such deficiencies highlighted the need for formulation
83 optimization of a capsule filling that was compatible with the polymeric walls. Also desirable,
84 and explored in the current study, is a 3D printable modular system capable of including larger
85 numbers of molecules and controlling their dissolution rate.

86 Physiologically based pharmacokinetic (PBPK) model simulation is a tool which has been
87 increasingly used in pharmaceutical development in order to improve efficiency and reduce costs
88 in drug development and absorption, distribution, metabolism & excretion (ADME) assessments.
89 It has proved useful in optimization of clinical trials design, for example in the selection of the
90 drug dose, and helped to understand how individual variability affects drug pharmacokinetics.
91 The simulation model has also demonstrated to be a valuable tool in clinical trials that need
92 individualized adjustable drug doses, for example paediatric^[32] and hepatically impaired
93 patients.^[33]

94 In this study, we present a facile modular platform for individualized complex therapeutic
95 regimens. By adopting combined hot-fill technology to produce unibody capsules of complex
96 structure, a highly modular capsule platform with tuneable release was achieved by mere use of
97 a modified digital design. Four model drugs were used in the development of two highly flexible
98 systems. The first system was based on manipulating pore size in a water insoluble biodegradable

99 shell (polylactic acid (PLA)). The second system was based on shell thickness control of a water
100 soluble PVA shell. The *in-silico* simulation of pharmacokinetics of these tablets aimed to provide
101 a means of pre-designing optimization of the pharmacokinetics of multiple drugs to suit individual
102 patient need.

103 2. Results and discussion

104 Capsules of complex structure were designed to include an oval hollow geometry comprising 4
105 compartments, where each compartment accommodated a single drug-loaded capsule filling. The
106 compartments were configured in two design formats (parallel or concentric) to achieve different
107 drug release patterns. Each design was split into two complementary parts: top and bottom design
108 files (correspondent to the base and cap) (**Figure 1**). The design allowed for three-step
109 manufacturing, where the base of the capsules was produced first (**Figure 2A3 and 2B3**), then
110 hot-filled (**Figures 2A4 and 2B4**) before, thirdly, a complementary cap is printed with subsequent
111 sealing of the capsule (**Figure 2A5 and 2B5**). After dispensing the identical volume of the filling,
112 it reached similar height within the capsule. The physical isolation of each drug in a separate
113 compartment is considered to prevent potential drug-drug interactions within the dosage form and
114 allow for the individualization and “tuning” of each model drug’s release profile.

115 Parallel compartments were designed into the capsular structure with different pore sizes,
116 according to the desired release profile (**Figure 1A**). Internal compartments were designed with
117 (2 mm) free-pass windows to yield an immediate release profile whilst external compartments
118 were fabricated with rate-limiting pores to extend drug release from the capsule. Following an
119 optimization process of pore configuration, dual pores for each side of the compartment seem to
120 allow faster drug release than a single pore of double size (**Supporting information, Figure S1**).
121 The impact of pore size on drug release was also screened for all module drugs (**Supporting**
122 **information, Figure S2**). Finally, total pore surface areas of 0.25 mm² and 0.49 mm² for each
123 compartment were selected to offer an extended release (**Figure 1B4**). The inclusion of four
124 identical square-shaped pores with a total area of 0.25mm² and 0.49mm² for each compartment

125 permitted aqueous flow within the capsule. SEM images confirmed pore walls within a range of
126 $\pm 60 \mu\text{m}$ of the design (data not shown).

127 To obtain extended and delayed drug release profiles, an alternative format (concentric capsule)
128 was devised. Two external and two internal compartments were configured to obtain extended
129 and delayed drug release profiles, respectively (**Figure 1B**). A wall thickness of 0.6 mm was
130 selected to maintain physical integrity of the capsule. By manipulating the thickness of the
131 bottom, upper and inner walls of the two inner compartments, the design aimed to control the lag
132 time of the delayed drug release. Capsules of different thickness of the inner wall (in multiple
133 increments of 0.6 mm) were fabricated to probe their effectiveness in delaying drug release
134 (**Figures 2A1/2/6**).

135 In order to establish the modularity of the system to meet various patients' needs, both design
136 formats were configured in two drug-sequences: Sequence I, where the most soluble drugs
137 (lisinopril and amlodipine) are dispensed in the immediate (PLA shell) or extended (PVA shell)
138 release compartment and the least soluble drugs (indapamide and rosuvastatin) were placed in the
139 extended (PLA shell) or delayed (PVA shell) release compartments. Sequence II differed in that
140 the model drugs were configured in reverse order.

141 Liquid infill formulations are often used in capsules to improve solubility or the dissolution of
142 poorly soluble drugs.^[34] Putting a liquid formulation into a 3D printed capsule shell presents a
143 major challenge with reported leaking issues and loss of capsule structure.^[31] To establish
144 compatibility between the infill *versus* the PVA and PLA 3D printed capsule shells, a fluorescent
145 molecule was used in the hot fill process of a liquid formulation of PEG 400, a commonly used
146 solubility enhancer in soft gelatine capsules.^[35, 36] Photographs of PVA concentric capsules
147 showed the absorption of the PEG solution by the shell through time (**Figure 3A**). Indeed,
148 microscopic pictures confirmed the migration of fluorescent solution through the polymeric shell
149 in contact with the PEG solution. This could be attributed to the established miscibility of PEG
150 400 with the PVA matrix.^[37] Likely arising from the significant known plasticising effect of PEG
151 ^[38], capsule shell deformation and compromised physical integrity were observed. Uncontrolled,

152 this could lead to interference of the different drug-loaded fillings and alter the individualized
153 release patterns of the drugs as well as initiating potential drug-drug interactions. On the other
154 hand, PLA capsules remained visibly unchanged with PEG solution as the capsule filling (**Figure**
155 **3B**). However, a previous study has reported the plasticising effect of PEG 400 in PLA when
156 mixed at 90 °C. ^[39]

157 To overcome this, PEG 4000 (melting temperature of 61. 5°C,) was added to allow solidification
158 of the structure at room temperature (**Figures 4E/F/G/H**). The paste was engineered to solidify
159 rapidly within the capsule compartments. Our initial screening indicated that an overall
160 percentage of PEG blends is ideal around 40% to maintain the integrity of the shell e.g. an
161 increased ratio of PEG 400 yielded fillings that leaked and were not compatible with the shell,
162 while fillings with increased ratio of PEG 4000 were too slow to solidify and compromised the
163 shell integrity (data not shown). *In order to regulate the rheological behaviour during extrusion,*
164 *lactose was added to the blend and yielding a facile filling paste to be hot-filled at relatively low*
165 *temperature (60 °C).* Thermogravimetric analysis was performed in order to assess thermal
166 stability of the raw materials and the developed drug-loaded capsule fillings. Thermogravimetric
167 profiles of drug-loaded capsule fillings showed continuous weight loss of about 3% up to 120 °C,
168 which was believed to be due to evaporation of moisture in the PEG 400, PEG 4000 and drug
169 substance (**Figure 4 A/B/C/D**). No significant weight loss was observed at the processing
170 temperature (60 °C).

171 The stability of the drug in the fill matrix was determined after 24 hrs to assess the compatibility
172 of the model drugs at the processing conditions temperature. All individual capsule fillings
173 showed a good stability at the processing temperatures for a period of at least 24 hrs (data not
174 shown), a finding indicating that the composition would be compatible with a process automation
175 using dispensing heated syringes.

176 Considering the results of differential scanning calorimetry, the presence of the endothermic
177 peaks corresponding to the melting of a blend of PEG 400, PEG 4000 and lactose for the drug-
178 free and drug-loaded capsule fillings, confirms the presence of crystalline components, which

179 facilitates their solidification on dispensing to the capsule shell. A broad peak is seen in both drug-
180 free and drug-loaded capsule fillings in the range of 100-150 °C, that may be explained by
181 dehydration of lactose (**Figure 4**). The DSC profile for the lisinopril-loaded capsule filling
182 suggested degradation at around 150 °C. This finding was not unexpected given the reported
183 sensitivity of this molecule to degradation through a Maillard reaction with lactose (**Figure 4E**).
184 ^[40] The use of 60 °C as a processing temperature will minimise the interaction.

185 XRD intensity patterns of the lisinopril-loaded capsule filling showed diffraction peaks
186 characteristic of the drug substance at $2(\Theta) = 7.5^\circ$, 12.5° and 13.6° , revealing the presence of the
187 crystalline form of the drug (**Figure 5A**). The absence of characteristic diffraction peaks of
188 amlodipine, indapamide and rosuvastatin in their correspondent capsule filling indicates that these
189 drug substances were likely amorphous within capsule fill matrices (**Figures 5B-D**). This finding
190 was consistent with DSC data, which revealed no endothermic events near the melting
191 temperatures of any of the drugs. These findings could be partially explained by the solubility
192 parameters values of PEG and the model drugs (**Table 2**). Lisinopril and amlodipine showed the
193 highest discrepancy in total solubility parameter value in comparison to PEG, while rosuvastatin
194 and indapamide have solubility parameter values with a difference of $<7 \text{ MPa}^{1/2}$.

195 While PEG 400 serves as solvent, PEG 4000 and lactose were added to increase the viscosity of
196 infill upon cooling to room temperature. Therefore, rheology studies were performed to confirm
197 the functionality of PEG 4000 and lactose in the capsule fillings as viscosity enhancers. This will
198 allow to assess the flowability of the filling at various temperatures and identify the ideal
199 temperature for capsule filling. The viscosity of the filling was assessed at various temperatures.
200 Complex viscosity data at the processing temperature (50 °C) are shown in **Figure 5E**. (Attempts
201 to assess the complex viscosity of the samples at room temperature (25 °C) were unsuccessful,
202 due to the solid nature of the ink). The minimum temperature that allowed successful analysis
203 was 40 °C and results can be seen in **Figure 5F**. The results show that PEG 400 has a relatively
204 low viscosity with minimum shear thinning behaviour (typical Newtonian fluid). On the other
205 hand, PEG 4000 has the highest complex viscosity value with a more pronounced shear thinning

206 behaviour typical of thermoplastic polymers. Their mixtures exhibited a complex value in
207 between both the pure material with shear thinning behaviour. The addition of lactose increased
208 the complex viscosity value while maintaining the shear-thinning behaviour. In general, adding
209 model drugs to each formulation did not have a significant effect on the complex viscosity
210 (complex viscosity studies for other model drugs are shown in **Supporting information, Figure**
211 **S3**).

212 The strategy of pore fabrication via FDM 3D printing can influence drug release profiles. Initially,
213 drug release from the capsule was attempted through inclusion of a single perforating square
214 shape (pore), however drug release was limited. To accelerate drug release, a dual pore system
215 was employed for each compartment. The effect on drug release was markedly evident compared
216 to a single pore, despite having the same total area (**Supporting information, Figure S1**). The
217 increase was attributed to an enhanced hydrodynamic flow through the capsule in the dual pore
218 system, leading to accelerated media flow and a thinner dissolution layer. It is also possible that
219 air bubbles can be entrapped within the compartment and hinder hydrodynamic flow within the
220 compartment. Therefore, this risk was mitigated by using four rate-limiting pores per
221 compartment.

222 Different pore areas were then evaluated (**Supporting information, Figure S2**). In general, an
223 increase in the total area pore area resulted in faster release rate of the drugs. However, controlling
224 release by modification of the pores area proved to be more effective with indapamide and
225 rosuvastatin, which have lower aqueous solubilities, when compared with lisinopril and
226 amlodipine.^[41-44] Total areas of 0.25 and 0.49 mm² provided a better extended release for lisinopril
227 and amlodipine, and indapamide and rosuvastatin, respectively. In Sequence I, lisinopril and
228 amlodipine showed an immediate release with >80% of drug dissolved in 30 min. A total pore
229 area of 0.49 mm² was necessary to achieve 89% and 55% of indapamide and rosuvastatin release
230 after 24 hrs (**Figure 6A2**). The effect of drug solubility was visually demonstrated by comparing
231 with Sequence II, where the free-pass corridors allowed >80% of indapamide release only after 3
232 hours (**Figure 6B**). An increase in the dissolution rate after pH change at 2 hrs was observed for

233 rosuvastatin and indapamide which can be explained by their acidic nature (pKa of 4.2-4.6 and
234 8.8 respectively).^[45, 46] Although a 0.49 mm² area proved to be suitable to reach extended release
235 in Sequence I, a smaller area (of 0.25 mm²) was necessary to slow down lisinopril and amlodipine
236 release (**Figure 6B1**). This illustrated the importance of software input to “tune” drug release
237 through pore size to accommodate a wide range of model drugs of variable solubilities.
238 Incomplete drug release was observed for indapamide and rosuvastatin in **Figures 6A1/A2** and
239 for lisinopril and indapamide in **Figure 6B1**, after a period of 24 hrs. This might lead to higher
240 plasma exposure when patients have longer transit time.^[47] Therefore, it is important to engineer
241 capsules to complete drug release within the transit time of non-disintegrating oral doses.

242 In order to achieve a chronotherapeutic effect, a concentric PVA polymeric shell was devised.
243 The design was successful in producing extended and time-dependent delayed release (**Figure 7**).
244 In general, a thickness of 0.6 mm was responsible for a lag time of 1 hr, and drugs dispensed in
245 the external compartments achieved >75% of drug released after approximately 3 hours after the
246 start of dissolution (**Figure 7**). This lag phase can be attributed to the time needed for the
247 dissolution of the outer shell and drugs in the external compartments. The dissolution mechanism
248 of PVA in the capsule shell is mediated mainly through erosion.^[48,49] Increasing the inner, top and
249 bottom walls thicknesses to 1.2, 1.8 and 2.4 mm resulted in a lag time of ~ 4, 6 and 8 hrs,
250 respectively, and >80% drug dissolution around 6 hrs thereafter (**Figure 7A3/B3**). External
251 compartments (of 0.6 mm thickness) eroded at a speed of 0.6 ± 0.0 mm/hr, and internal
252 compartments at 0.41 ± 0.09 mm/hr. The suitability of the polypills was demonstrated using four
253 clinically relevant drugs for the treatment of CVD, however its application to other therapeutic
254 regimens is unlimited. The high versatility of the system is expected to be associated with
255 improved clinical outcomes, by customization of the release profile of drugs to target specific
256 times to attain peak plasma concentration and to avoid drug-drug interactions in complex
257 therapies. One limitation of the developed capsule systems is its relatively large size and shape.
258 Further reduction of the capsules size and a transformation to capsule-like geometry could be

259 applied to meet FDA guidance for recommended size and shape in order to improve patient
260 acceptability.^[50]

261 In the clinical setting, bespoke dosage forms can be dispensed as a patient-specific medicine in
262 an extemporaneous setting. Initial stability trials to determine the impact of storage conditions of
263 the developed capsules were conducted over 28 days. In general, no physical change of the
264 capsule structure was observed by visible inspection (**Supporting information, Figure S4**).
265 Lisinopril and rosuvastatin did not show significant ($p>0.05$) degradation when stored at 4°C
266 (**Supporting information, Table S1**), while a decrease in drug content was significant ($p>0.05$)
267 for indapamide and amlodipine when in PLA capsules. This may be explained by a protective
268 effect of the PVA shell on moisture. The highest degree of degradation of amlodipine when
269 compared with the rest of the model drugs may be due to the high sensitivity of this drug molecule
270 to moisture and light.^[51,52] It is possible that the open pores within the architecture of the parallel
271 design favoured the penetration of light and moisture and contributed to higher level of
272 degradation in amlodipine chamber. In general, immediate release chambers yielded similar
273 release pattern, whilst extended and delayed release patterns was more sensitive to storage
274 temperature (**Supporting information, Figures S5 and S6**).

275 To project the clinical implication of using this bespoke drug delivery system for cardiovascular
276 system, a simulation absorption model was developed to study the effect of drug
277 dissolution in drug pharmacokinetics. Validation of the developed models was performed by
278 comparison of the simulated AUC, C_{max} and T_{max} with the observed clinical studies (**Supporting**
279 **information, Table S2**). PLA-based capsules showed a clear predictable effect of drug
280 dissolution in the pharmacokinetics profile. C_{max} was proportional with the maximum drug release
281 achieved from the *in vitro* dissolution studies (**Figure 8 and Supporting information, Figures**
282 **S7**). PVA-based concentric capsules with different wall thicknesses showed similar good
283 correlation with C_{max} values and T_{max} values proportionally increasing with the drug release time
284 (**Figure 9 and Supporting information, Figures S8**). Pharmacokinetic parameters values
285 obtained for PLA and PVA capsule systems can be found in **Supporting information, Table S3**

286 **and S4**, respectively. The ease of modelling the results highlights the applicability of such a
287 highly modular drug delivery systems to conveniently produced timed drug dose release with
288 “tuned” peak drug plasma concentrations to achieve optimal clinical outcome.

289 We envisage the employment of such digitised and modular system as part in an integrated
290 healthcare network in the future (**Figure 10**). In such a configuration, patient’s data and genomics
291 will feed an artificial intelligent and big data-powered network, where desired target PK profile
292 can be set, tested and refined in multiple cycles to achieve clinical outcome in seamless fashion.
293 The growth of database and number of participants in such integrated system to a critical mass
294 can potentially revolutionise and transform the efficacy, safety and patient-centricity of multiple
295 drug treatments.

296 3. Conclusions

297 We present a highly modular multi-compartmental capsule platform of complex structure that
298 accommodates 4 model drugs for bespoke dosing and drug release. A specially developed rapid
299 solidifying fill matrix proved compatible with two biodegradable polymeric shells (PVA and
300 PLA). Two architecture formats, based on digital manipulation of wall thickness and pore sizes,
301 allow a customised release profile for each drug molecule. The novelty of this system resides in
302 employing an established additive manufacturing method with liquid dispensing to achieve a
303 complex multidrug releasing dosage form starting from identical materials. Hence, the platform
304 enables serving large number of patients with a small number of starting materials and relatively
305 low costs. The approach yields minimal migration of the formulation through the shell structure
306 and is stable for 28 days following production (comparable to the usual shelf-life for
307 extemporaneous preparations). While this work provides a proof-of-concept for 4 drug molecules,
308 the reported platform can easily be generalised to a wider spectrum of drug substances that are
309 frequently prescribed together. This work showcases a powerful and economical approach of
310 digital design to provide healthcare staff with a highly adjustable ‘polypill’ solution, to

311 accommodate the increasing number of patients who receive multiple and complex dosing
312 regimens.

313 **4. Experimental Section**

314 *Materials:* Lisinopril dihydrate, amlodipine besylate, indapamide and rosuvastatin calcium
315 were obtained from Kemprotec Ltd (Cumbria, UK). HPLC gradient grade acetonitrile and
316 methanol were from Fisher Scientific Ltd (Loughborough, UK). Dipyridamole, poly(ethylene
317 glycol) (PEG) 4000 and alpha-D-Lactose monohydrate ACS reagent grade were purchased from
318 Thermo-Fisher Scientific (UK). Poly(ethylene glycol) (PEG) 400 was from Merck KGaA
319 (Darmstadt, Germany). Polyvinyl alcohol (PVA) and Poly(lactic acid) (PLA) filaments were
320 obtained from MakerBot® Industries (NY, USA). All other chemicals were of analytical grade.

321

322 *Preparation of the capsule fill matrix:* A rapid solidifying shell-compatible hot-fill fluid was
323 developed. The composition of each drug-loaded fill matrix is detailed in Table 1. The filling
324 was prepared by dissolving accurately weighed model drug in PEG 400 in a beaker and sonicating
325 the solution/suspension for 15 min. PEG 4000 was then incorporated in the mixture, which was
326 then heated in a FD240 binder heating chamber (Tuttlingen, Germany) for 1 hr at 60°C. Following
327 the complete melting of PEG 4000 and mixed, lactose was suspended and manually mixed to
328 obtain a uniform paste. Pastes were then maintained at 50°C. A volume of 80 µL (~100 mg) of
329 each model drug fill matrix was manually dispensed in each capsule compartment using a 1-mL
330 GASTIGHT® syringe (Hamilton Company, UK) equipped with a 18 gauge- 6.35 mm length
331 needle (McMaster-Carr, CA, USA).

332

333 *3D printing of capsules:* Capsule shells of innovative complex architecture were designed using
334 Autodesk® 3ds Max Design 2016 software version 18.0 (Autodesk, Inc., USA). An oval shape
335 was chosen to simplify its division into 4 compartments with similar volumes. The capsules (with
336 0.6 mm walls) were designed with a standard size of 24.1 x 15.1 x 6.26 (X x Y x Z) mm. PVA

337 capsules were designed with z dimension of 7.46, 8.66 and 9.86 mm for designs with inner wall
338 thickness of 1.2, 1.8 and 2.4 mm respectively. Two design formats (**Figure 1**) were adopted to
339 couple extended or delayed release patterns for two model drugs with immediate or extended
340 release for the other two model drugs:

341 1. *PLA-based parallel design capsules with immediate release and extended release*
342 *architecture (Figure 1A)*. Internal compartments were designed with free-pass corridors
343 (2 mm) to facilitate free access of dissolution media and subsequent rapid dissolution and
344 release of capsule fillings. External compartments were designed with rate-limiting pores.
345 The optimization of the design was performed by assessing the release profile of the drugs
346 using a different number (two or four) of the rate-limiting pores per compartment and
347 different total pore areas (namely, 0.25, 0.49, 0.72 and 1mm²). After optimization, the
348 design with four pores per external compartment (two on each side) and pores areas of
349 0.25 and 0.49 mm² were selected as a default.

350 2. *PVA-based concentric design capsules with variable shell thicknesses (Figure 1B) with*
351 *extended and delayed release system architecture*. External walls of the capsule were
352 designed with a 0.6-mm thickness to provide an extended release. Capsules with top,
353 bottom and internal walls were designed with various wall thicknesses (namely 0.6, 1.2,
354 1.8 or 2.4 mm) in order to achieve a delayed drug release profile from the internal
355 compartments.

356 Each design was split into two complementary objects: cap and base. 3D printing of both capsule
357 formats was done using a Makerbot Replicator 2X (Makerbot Industries, LLC, USA) at nozzle
358 and platform temperatures of 200 °C and 50 °C, respectively. Capsule shells were divided in two
359 stereolithography (.stl) files format correspondent to the base and cap of the capsule. 3D printing
360 of the capsule shells was performed without using removable supports and took a maximum of
361 10 min. Each capsule was fabricated in three steps: i) 3D printing of the bottom portion of the
362 design (**base**), ii) manual capsule filling as detailed in the previous section, and iii) 3D printing of
363 complementary top part (**cap**). The printing of cap was set using the identical x-y position on the

364 printing plate and at z-level equivalent to the height of the complementary base. No additional
365 sealing materials or process were used in the process.

366 *Compatibility of the hot-filling matrix with the capsule shell:* Fill-matrix compatibility with PLA
367 and PVA shells was studied by assessing the developed fast solidifying fills using a fluorescent
368 molecule (dipyridamole). Capsule fillings (as described above) and dipyridamole solution in PEG
369 400 (control) were dispensed in PLA and PVA capsules and visualised in a NOVEX B-range
370 microscope after 0, 0.5, 2 and 24 hrs. Samples were prepared using the concentration
371 correspondent to the model drug with lowest dose (indapamide), 31.25 mg/mL and 2.5% for the
372 PEG 400 and capsule filling samples, respectively. The capsules were kept at room temperature
373 throughout the experiment and images were obtained using Image focus v3.0.0.1 software to
374 visualise integrity.

375 *High performance liquid chromatography (HPLC):* Drug content and dissolution tests samples
376 were analysed by HPLC, using a method that has been described in a previous study.^[53]

377 *Thermal analysis:* Thermogravimetric analysis (TGA) analysis was performed on a TGA Q500
378 (TA Instruments, Elstree, Hertfordshire, UK) and samples of the raw materials and the capsule
379 fill matrix were run in triplicate. Each sample (approximately 10mg) was heated at a rate of
380 10 °C/min from 25 to 500 °C with a nitrogen purge of 40:60 mL/min for sample: furnace
381 respectively. Differential Scanning Calorimetry (DSC) analysis was conducted on a DSC Q2000
382 (TA Instruments, Elstree, UK). Samples (~10 mg) of the raw materials and the capsule fill matrix
383 were analysed in triplicate using T-zero hermetic pans. Each sample was scanned from -50 to
384 230 °C at 10 °C/min using a nitrogen purge of 50 mL/min. Data obtained from both TGA and
385 DSC were analysed with TA Universal analysis software v4.5A (TA Instruments, Elstree, UK).

386

387 *Powder X-ray diffractometry (XRD):* Powder XRD analysis of the raw materials and capsule
388 filling was carried out using an X-ray diffractometer, D2 Phaser with Lynxeye (Bruker,
389 Germany). Each sample was scanned from $2\theta = 5^\circ$ to 50° with a 0.01° step width and a 1.25 sec

390 time count. The divergence slit and scatter slit were 1 mm and 0.6 mm, respectively. The
391 wavelength of the X-ray was 0.154 nm using a Cu source, a voltage of 30 kV and a filament
392 emission of 10 mA.

393

394 *Rheological studies of the capsule fill matrix:* Rheology studies were performed on the capsule
395 fills using an Anton Paar Shear Rheometry Physica MCR 301 (Graz, Austria) with 25mm parallel
396 plates, using a 0.5mm gap distance in oscillation mode. Linear viscoelastic region (LVR) was
397 studied with 0.5% strain amplitude. Samples were tested in triplicate using an amplitude sweep
398 at an angular frequency range from 0.1 to 100 rad/s and angular frequency of 10 rad/s.
399 Temperatures were set at 40 and 50°C (dispensing temperature) and readings were collected every
400 5 sec.

401 *Solubility parameter:* Hansen solubility parameters were calculated using HSPiP v5.0.08
402 software. The canonical simplified molecular-input line-entry system (SMILES) of the
403 compounds as stated in ^[54] was used to calculate the solubility parameters using group
404 contribution method. It is worth noting that PEG 400 and PEG 4000 have identical SMILES and
405 therefore have identical solubility parameter values.

406 *Stability assessment:* The stability of the developed formulation was assessed in terms of
407 compatibility with the capsule shells, drug content and dissolution profile. The drug content
408 (w/w%) of each capsule filling was calculated by comparing the recovered amount with the
409 theoretical amount.

410 *a. Stability at processing conditions:* To mimic the impact of the temperature of capsule
411 filling on model drug integrity, drug contents of capsule fill pastes (stored in syringe)
412 were assessed at 50 °C in a FD240 Binder heating chamber (Tuttlingen, Germany).
413 Samples were collected at the time points 0 and 24 hrs, filtered through an Econofltr 0.2
414 µm syringe filter (Agilent Technologies Ltd., Cheshire, UK) and analysed in triplicate by
415 the HPLC method mentioned above.^[53]

416 *b. Accelerated stability study:* Accelerated stability of the 3D printed capsules (Sequence I
417 PLA-based capsules with 0.49 mm² pores and Sequence I PVA-based capsules with 1.8
418 mm wall thickness) was performed according to ICH guidelines for one month, at 4 °C,
419 30 °C/ 65% RH and 40 °C / 75% RH. Capsules were individually stored in high-density
420 polyethylene bottles and analysed in triplicate in terms of visual assessment of physical
421 capsule structure, drug content and dissolution profile (see above). For drug content
422 analysis, PVA capsules were placed in 800 mL of water and sonicated until complete
423 dissolution, followed by the addition of 200 mL of acetonitrile and further sonication for
424 1 hr. PLA capsules were firstly dissolved in 200 mL of acetonitrile followed addition of
425 800 mL water and sonication for 1 hr. For amlodipine analysis, 1 mM EDTA was added
426 the solution. The solutions were then filtered through an Econofltr 0.2 µm syringe filter
427 (Agilent Technologies Ltd., Cheadle, UK) and analysed by HPLC as described above.

428 *Scanning electronic microscopy (SEM)* The thickness of the inner wall of the PVA concentric
429 capsules and the pores of the PLA capsules were analysed with a JCM-6000 plus NeoScope™
430 microscope (Jeol, Tokyo, Japan) at 10 kV. Prior to imaging, samples were gold coated under
431 vacuum for 2 min with a JFC-1200 Fine Coater (Jeol, Tokyo, Japan).

432 *In vitro dissolution tests.* The dissolution tests for 3D printed capsules were performed on an
433 Erweka DT600 USP II dissolution test apparatus (Heusenstamm, Germany). The tests were run at
434 37 °C with a paddle rotation speed of 50 rpm, under sink conditions. The capsules were tested in
435 750 mL of 0.1M HCl (pH 1.2) for 2 hrs, followed by pH 6.8 phosphate buffer for 4 hrs (with
436 addition of 250 mL of tribasic phosphate solution 0.215 M) and then pH 7.4 phosphate buffer for
437 additional 18 hrs. The paddles and the water bath were sealed with PTFE-coated glass cloth
438 adhesive tape (Viking Industrial Products, Keighley, UK) and foil, respectively, and the
439 dissolution assessment was performed in a dark room, to prevent degradation of amlodipine. Each
440 experiment was performed in repetitions of six and samples were manually collected (4 mL),
441 which was replaced and filtered with an Econofltr 0.2 µm syringe filter (Agilent Technologies
442 Ltd., Cheadle, UK). Aliquots were collected at the time points: 0, 0.5, 1, 1.5, 2, 3, 4, 5, 6, 8, 10,

443 12 and 24 hrs and analysed by the developed HPLC method previously described. The period of
444 24 hours was selected to cover the total transit time of non-disintegrating tablet (PLA based
445 capsule) in the gastrointestinal tract.^[55]

446 With the assumption that a detectable drug concentration is reached when the capsule wall is
447 completely dissolved, the erosion rate (mm/hrs) was estimated using the following equation:

$$448 \text{ Erosion rate} = d \text{ (mm)} / t_{\text{lag}} \text{ (hrs)}$$

449 where (d) is the thickness of the wall, and (t_{lag}) is the lag time before the onset of drug release.

450 *In silico simulation* The absorption profile simulation for each drug was developed using
451 Gastroplus® v9.7 (Simulation Plus, Lancaster, CA, USA). For the ‘compound’ and
452 ‘pharmacokinetics’ models, input data included experimental data (dissolution profile,
453 permeability and solubility) and data obtained from literature. When precise compound
454 parameters values were not available, parameter estimation was performed by the software.
455 Human physiology under fasted state mode was designated and default values were used.

456 The physicochemical properties and ADME parameters for each drug were obtained from
457 literature (**Supporting information, Table S5**).

458 *Statistical analysis* Statistical analysis of the results was done with independent t-test using SPSS
459 software (22.0.2). Differences in the results below the probability level of $p < 0.05$ were considered
460 significant.

- 461 [1] C.J. Charlesworth, E. Smit, D.S. Lee, F. Alramadhan, M.C. Odden, *J. Gerontol. A. Biol. Sci.*
462 *Med. Sci.* **2015**, 70, 989.
- 463 [2] B. Guthrie, B. Makubate, V. Hernandez-Santiago, T. Dreischulte, *BMC Med.* **2015**, 13, 15.
- 464 [3] E.R. Hajjar, A.C. Cafiero, J.T. Hanlon, *Am. J. Geriatr. Pharmacother.* **2007**, 5, 345.
- 465 [4] EHN, *European Cardiovascular Disease: Statistics 2017 edition*, in: S. Løgstrup (Ed.),
466 *Belgium*, **2017**.
- 467 [5] NICE, Cardiovascular disease risk assessment and prevention,
468 [https://bnf.nice.org.uk/treatment-summary/cardiovascular-disease-risk-assessment-and-](https://bnf.nice.org.uk/treatment-summary/cardiovascular-disease-risk-assessment-and-prevention.html)
469 [prevention.html](https://bnf.nice.org.uk/treatment-summary/cardiovascular-disease-risk-assessment-and-prevention.html), accessed: 8/2019.
- 470 [6] D. Cimmaruta, N. Lombardi, C. Borghi, G. Rosano, F. Rossi, A. Mugelli, *Int. J. Cardiol.*
471 **2018**, 252, 181.
- 472 [7] S. Assari, M. Bazargan, *Pharmacy (Basel)*, **2019**, 7, 14.
- 473 [8] S. Leszek, J. Jadwiga, B.-S. Agnieszka, *Ars Pharmaceutica*, **2016**, 57, 137.
- 474 [9] A. Atreja, N. Bellam, S.R. Levy, *MedGenMed*, 2005, 7,4.
- 475 [10] PillPack, Pill Pack, <https://www.pillpack.com/how-it-works>, accessed: 7/2019.
- 476 [11] NIHR, My medication passport, <http://clahrc-northwestlondon.nihr.ac.uk/resources/mmp>,
477 accessed: 7/2019.
- 478 [12] R.L. Padilla, S. Byers-Connor, H.L. Lohmam, *Occupational Therapy with Elders: Strategies*
479 *for the Cota.*, Second ed., Elsevier, USA, **2012**.
- 480 [13] A.D. Black, J. Car, C. Pagliari, C. Anandan, K. Cresswell, T. Bokun, B. McKinstry, R.
481 Procter, A. Majeed, A. Sheikh, *PLoS Med.* **2011**, 8, 1000387.
- 482 [14] J.M. Castellano, H. Bueno, V. Fuster, *Int. J. Cardiol.* **2015**, 201, 31027.
- 483 [15] S.E. Moulton, G.G. Wallace, *J. Control. Release.* **2014**, 193, 27.
- 484 [16] M. Alomari, F.H. Mohamed, A.W. Basit, S. Gaisford, *J. Pharm.* **2015**, 494, 56.
- 485 [17] A. Goyanes, F. Fina, A. Martorana, D. Sedough, S. Gaisford, A.W. Basit, *Int. J. Pharm.*
486 **2017**, 527, 21.
- 487 [18] K. Ilyes, N.K. Kovacs, A. Balogh, E. Borbas, B. Farkas, T. Casian, G. Marosi, I. Tomuta,
488 Z.K. Nagy, *Eur. J. Pharm. Sci.* **2019**, 129, 110.
- 489 [19] B. Arafat, N. Qinna, M. Cieszynska, R.T. Forbes, M.A. Alhnan, *Eur. J. Pharm. Biopharm.*
490 **2018**, 128, 282.
- 491 [20] N. Scoutaris, S.A. Ross, D. Douroumis, 3D Printed "Starmix" Drug Loaded Dosage Forms
492 for Paediatric Applications, *Pharm. Res.* **2018**, 35, 17.
- 493 [21] M. Sadia, A. Isreb, I. Abbad, M. Isreb, D. Aziz, A. Selo, P. Timmins, M.A. Alhnan, *Eur. J.*
494 *Pharm. Sci.* **2018**, 123, 484.
- 495 [22] C.I. Gioumouxouzis, A. Baklavariadis, O.L. Katsamenis, C.K. Markopoulou, N.
496 Bouropoulos, D. Tzetzis, D.G. Fatouros, *Eur. J. Pharm. Sci.* **2018**, 120, 40.
- 497 [23] T. Tagami, K. Fukushige, E. Ogawa, N. Hayashi, T. Ozeki, *Biol. Pharm. Bull.* **2017**, 40, 357.
- 498 [24] X. Chai, H. Chai, X. Wang, J. Yang, J. Li, Y. Zhao, W. Cai, T. Tao, X. Xiang, *Sci. Rep.*
499 **2017**, 7, 17.
- 500 [25] B. Arafat, M. Wojsz, A. Isreb, R.T. Forbes, M. Isreb, W. Ahmed, T. Arafat, M.A. Alhnan,
501 *Eur. J. Pharm. Sci.* **2018**, 118, 191.
- 502 [26] A. Melocchi, F. Parietti, G. Loreti, A. Maroni, A. Gazzaniga, L. Zema, *J. Drug Deliv. Sci.*
503 *Technol.* **2015**, 30.
- 504 [27] D. Smith, Y. Kapoor, A. Hermans, R. Nofsinger, F. Kesisoglou, T.P. Gustafson, A. Procopio,
505 *Int. J. Pharm.* 2018, 550, 418.
- 506 [28] G. Matijašić, M. Gretić, J. Vinčić, A. Poropat, L. Cuculić, T. Rahelić, *J. Drug Deliv. Sci.*
507 *Technol.* 2019, 52, 677.

- 508 [29] A. Maroni, A. Melocchi, F. Parietti, A. Foppoli, L. Zema, A. Gazzaniga, *J. Control. Release.*
509 **2017**, 268, 10.
- 510 [30] D.M. Smith, Y. Kapoor, G.R. Klinzing, A.T. Procopio, *J. Pharm.* **2018**, 544, 21.
- 511 [31] T.C. Okwuosa, C. Soares, V. Gollwitzer, R. Habashy, P. Timmins, M.A. Alhnan, *Eur. J.*
512 *Pharm. Sci.* **2018**, 118, 134.
- 513 [32] X.L. Jiang, P. Zhao, J. Barrett, L. Lesko, S. Schmidt, *CPT: pharmacometrics & systems*
514 *pharmacology*, **2018**, 2, 80.
- 515 [33] P.N. Morcos, Y. Cleary, C. Sturm-Pellanda, E. Guerini, M. Abt, M. Donzelli, F. Vazvaei, B.
516 Balas, N. Parrott, L. Yu, *J. Clin. Pharmacol.* **2018**, 58, 1618.
- 517 [34] M.A. Rahman, A. Hussain, M.S. Hussain, M.A. Mirza, Z. Iqbal, *Drug. Dev. Ind. Pharm.*
518 **2013**, 39, 1.
- 519 [35] S.S. Hong, S.H. Lee, Y.J. Lee, S.J. Chung, M.H. Lee, C.K. Shim, *J. Control. Release.* **1998**,
520 51, 185.
- 521 [36] P. Augustijns, M. Brewster, *Solvent Systems and Their Selection in Pharmaceutics and*
522 *Biopharmaceutics*, Springer/AAPS Press, New York, **2007**.
- 523 [37] F.H. Falqi, O.A. Bin-Dahman, M. Hussain, M.A. Al-Harathi, *Int. J. Polym. Sci.* **2018**, 10.
- 524 [38] L.Y. Lim, L.S.C. Wan, *Drug. Dev. Ind. Pharm.* **1994**, 1007.
- 525 [39] O. Martin, L. Avérous, *Polymer.* **2001**, 42, 6209.
- 526 [40] R. Eijolfsson, *Drug. Dev. Ind. Pharm.* **1998**, 24, 797.
- 527 [41] T.J. DiFeo, J.E. Shuster, Academic Press, *Indapamide. In: H. G. Brittain (Ed.) Analytical*
528 *Profiles of Drug Substances and Excipients*. Academic Press, USA, **1994**.
- 529 [42] N. Kulkarni, N. Ranpise, G. Mohan, *Trop. J. Pharm. Res.* **2015**, 14, 575.
- 530 [43] R. Dahima, A. Pachori, S. Netam, *Int. J. Chemtech. Res.* **2010**, 2.
- 531 [44] D.P. Ip, J.D. DeMarco, M.A. Brooks, *Lisinopril, in: H.G. Brittain (Ed.) Analytical Profiles*
532 *of Drug Substances and Excipients*, Academic Press, **1992**, pp. 233-276.
- 533 [45] D.T. Manallack, *Perspect. Medicin. Chem.* **2007**, 1, 25.
- 534 [46] M.V. Varma, C.J. Rotter, J. Chupka, K.M. Whalen, D.B. Duignan, B. Feng, J. Litchfield,
535 T.C. Goosen, A.F. El-Kattan, *Mol. Pharm.* **2011**, 8, 1303.
- 536 [47] C.G. Wilson, N. Washington, *Drug Dev. Ind. Pharm.* **2008**, 14,211.
- 537 [48] S. Vaddiraju, Y. Wang, L. Qiang, D.J. Burgess, F. Papadimitrakopoulos, *Anal. Chem.* **2012**,
538 84, 8837.
- 539 [49] J. Zhao, X. Xu, M. Wang, L. Wang, *Dissolution Technol.* **2018**, 25, 24.
- 540 [50] Center for Drug Evaluation and Research (CDER), FDA, Size, Shape, and Other Physical
541 Attributes of Generic Tablets and Capsules Guidance for Industry,
542 <https://www.fda.gov/media/87344/download>, accessed: 03/2020
- 543 [51] L. Malcolm, *Accelerated Predictive Stability (APS)*, **2018**, 287.
- 544 [52] F. Elisa, A. Angelo, G. Silvia, *Int. J. Pharm.* **2007**, 352, 197.
- 545 [53] B.C. Pereira, A. Isreb, R.T. Forbes, F. Dores, R. Habashy, J.B. Petit, M.A. Alhnan, E.F. Oga,
546 *Eur. J. Pharm. Biopharm.* **2019**, 135, 94.
- 547 [54] PubChem, <https://pubchem.ncbi.nlm.nih.gov/>, accessed: 9/2019.
- 548 [55] G. Sathyan, S. Hwang, S.K. Gupta, *Int. J. Pharm.* **2000**, 204, 47.

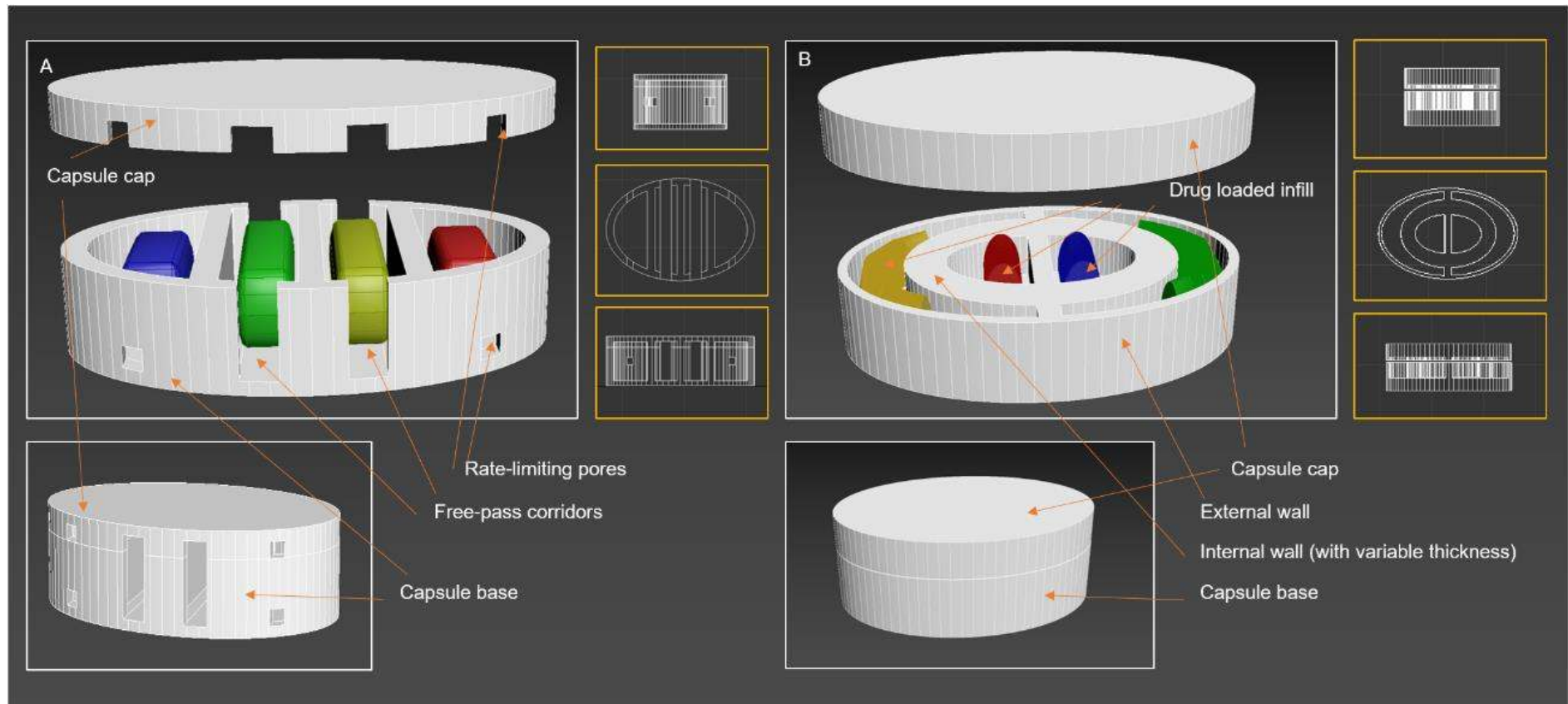


Figure 1 Rendered images of computer-aided design (CAD) (Autodesk 3DS Max) of capsule base and cap of (A) PLA capsules of parallel compartments with free-pass corridors and rate-limiting pores and (B) PVA capsules of concentric compartments design and varying internal wall thicknesses.

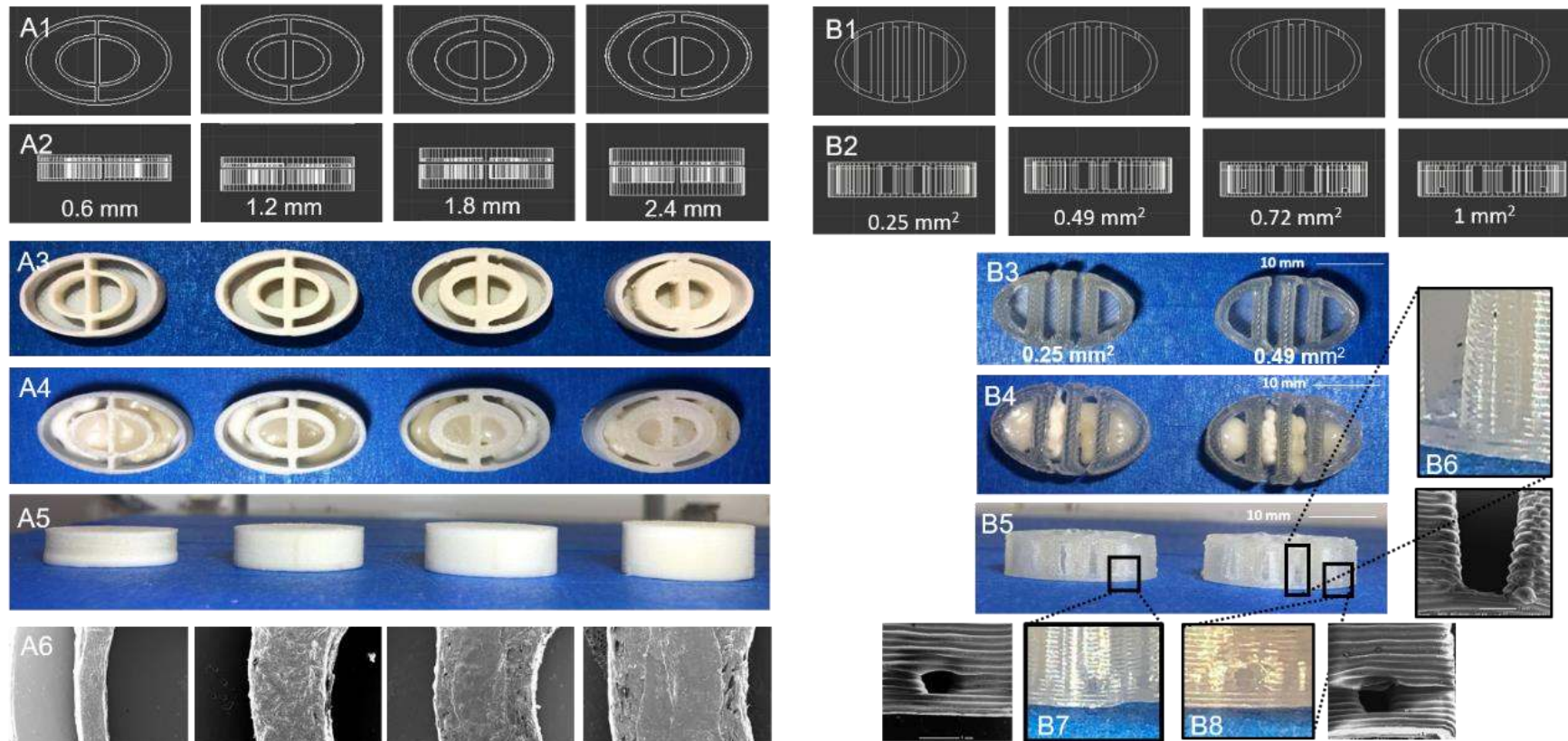


Figure 2 Schematic images of PVA capsules with increased thickness of (A1) inner wall and (A2) base and cap layers. Images of the PVA concentric design capsules (A3) 3D printed base, (A4) capsule filling, (A5) sealed capsules. (A6) SEM images of the inner wall with increased thickness. Images of PLA parallel design capsules (B1) printed base, (B2) capsule filling, (B3) sealed capsules. Detailed images and correspondent SEM pictures of rate-limiting pores with (B4) 0.25 mm² and (B5) 0.49 mm² areas and (B6) corridors from PLA capsules.

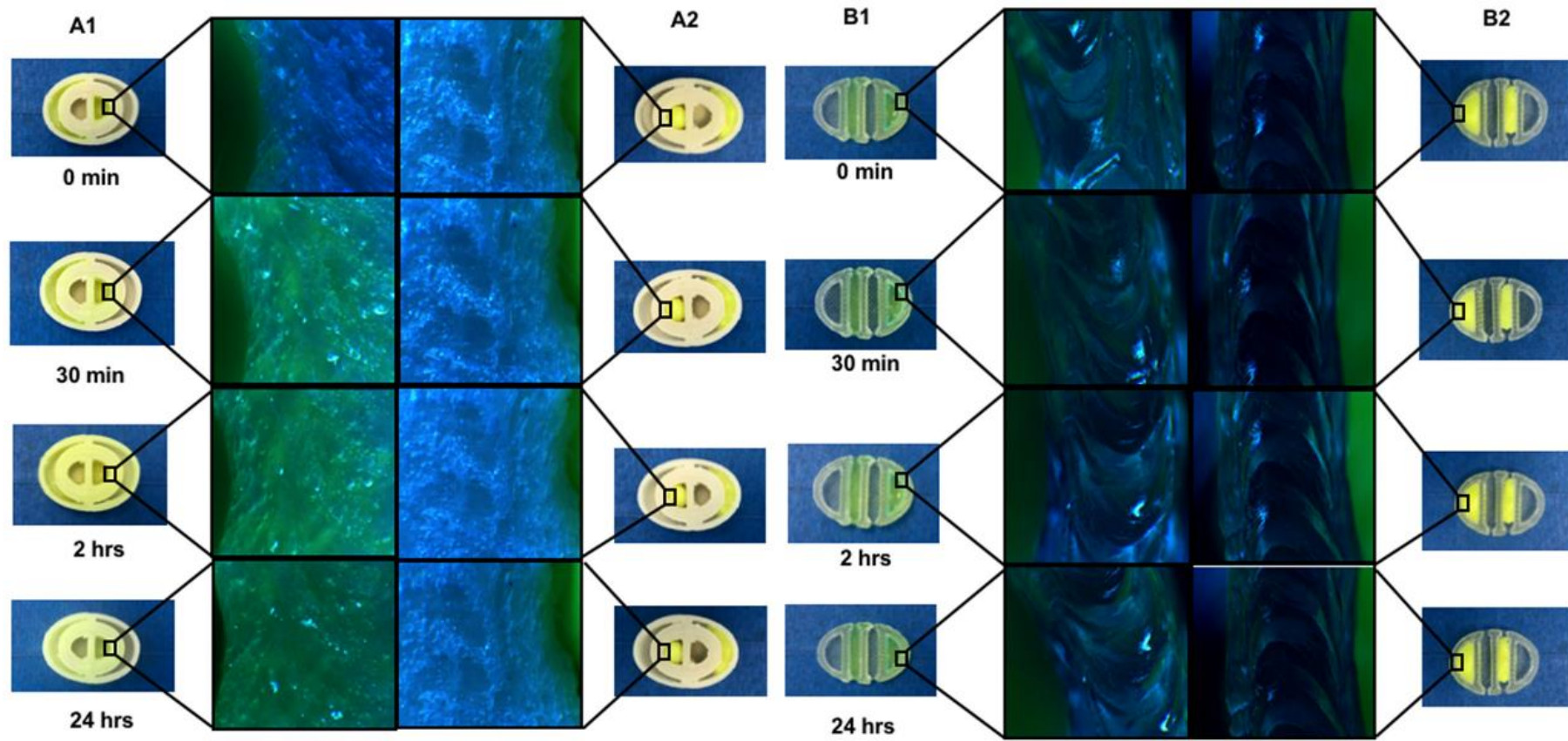


Figure 3 Images of (A1) PVA and (B1) PLA shells with dipyridamole PEG and (A2) PVA and (B2) PLA shells with dipyridamole-loaded capsule filling.

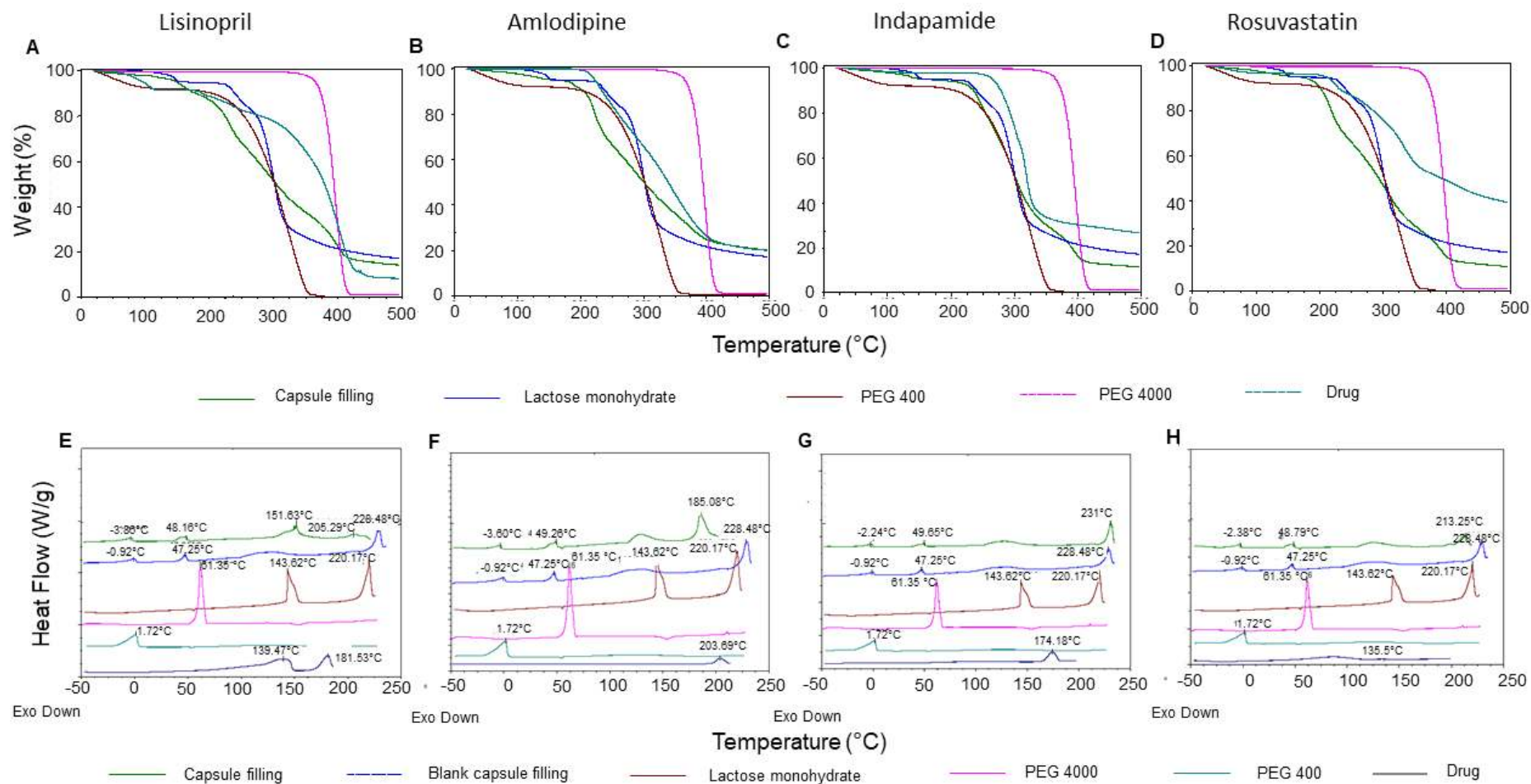


Figure 4 TGA profiles and DSC scans of raw materials and capsule filling of (A/E) lisinopril, (B/F) amlodipine, (C/G) indapamide and (D/H) rosuvastatin, respectively.

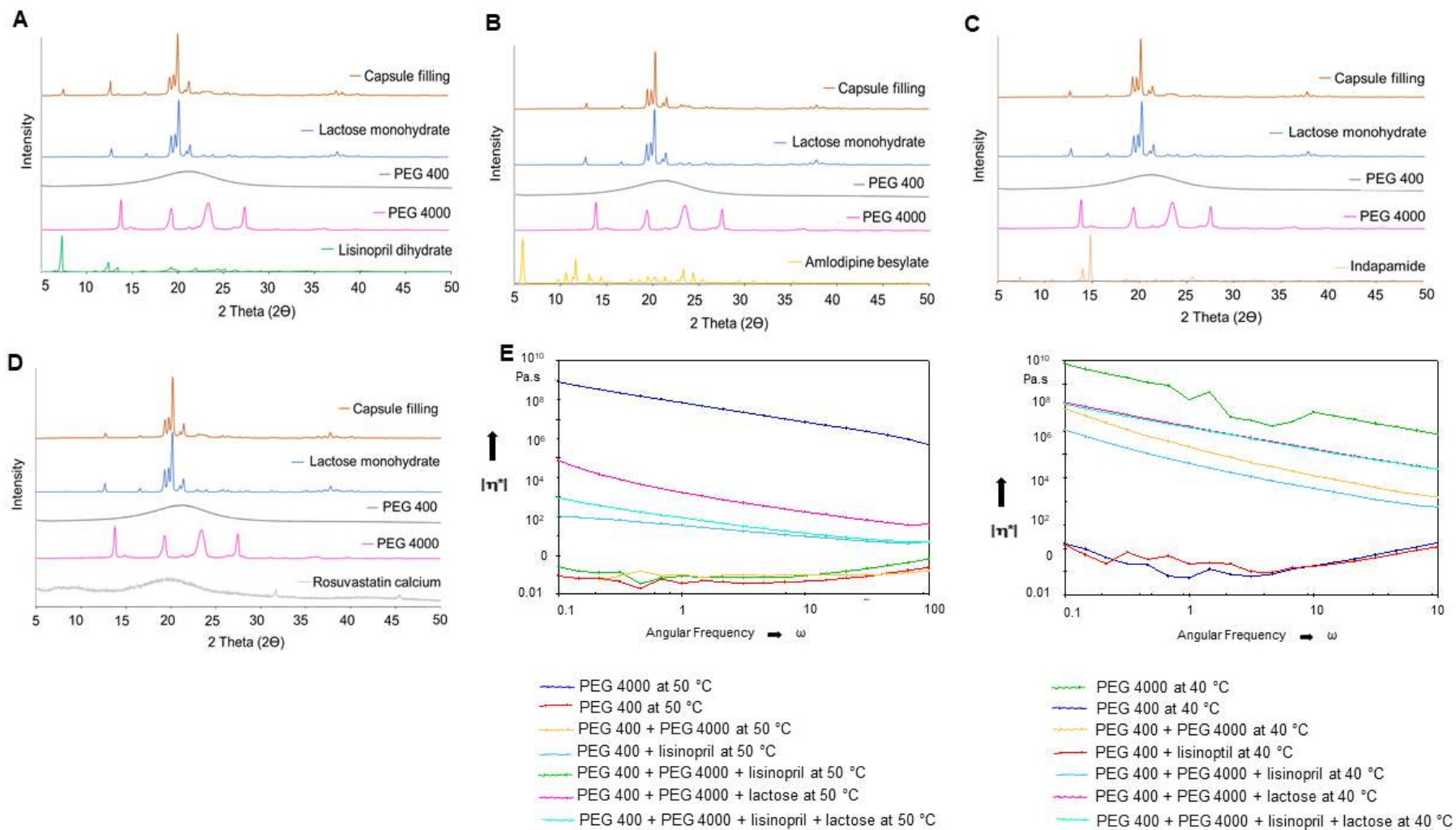


Figure 5 Powder XRD patterns of raw materials and capsule filling of (A) lisinopril, (B) amlodipine, (C) indapamide and (D) rosuvastatin. Complex viscosity of PEG 400, PEG 4000 and their mixtures with and without lactose and with lisinopril at (E) 50 °C and (F) 40 °C.

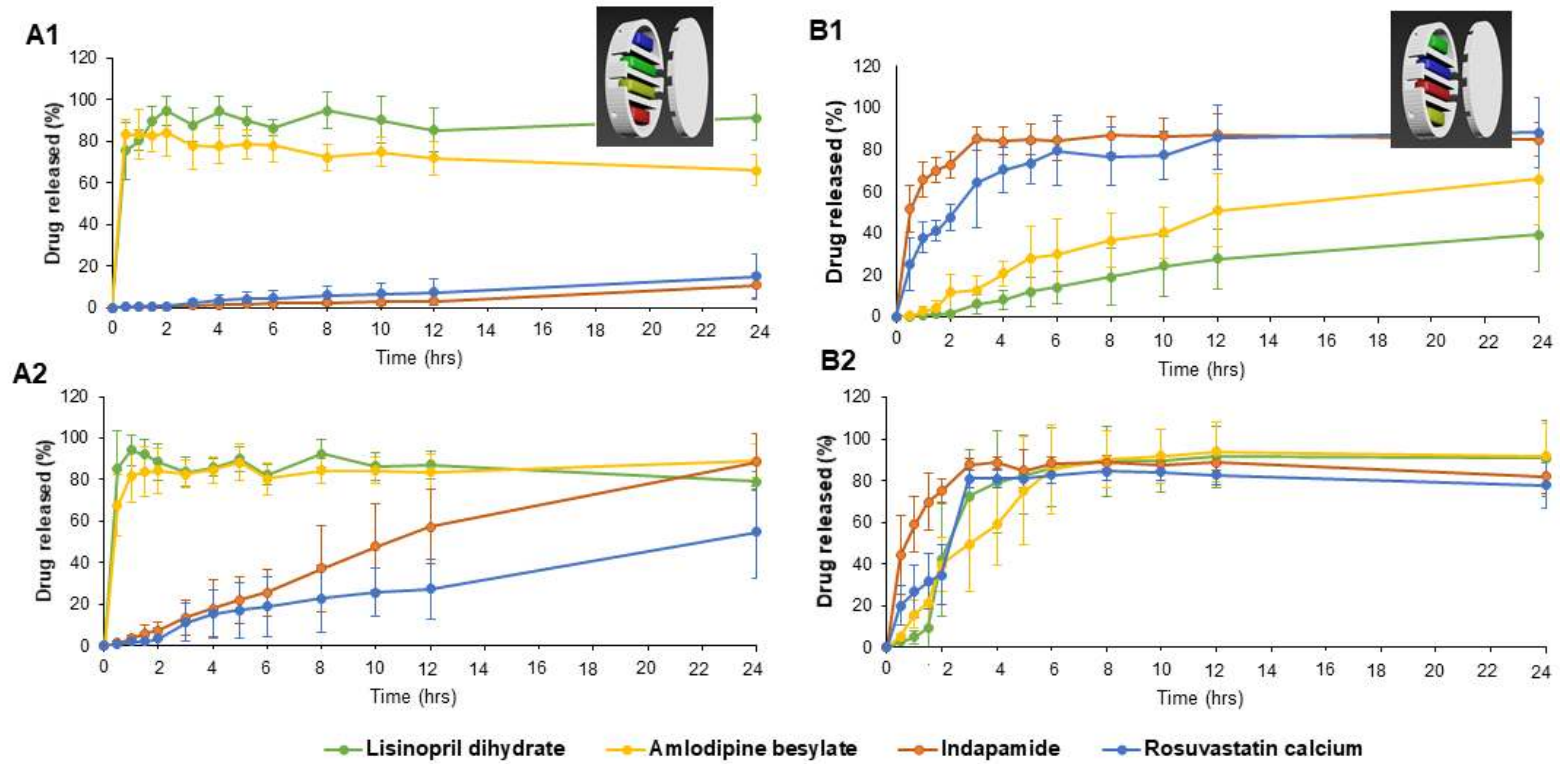


Figure 6 *In vitro* drug release of PLA parallel design capsules with (A1 and B1) 0.25 mm² pores and (A2 and B2) 0.49 mm² pores (n=6).

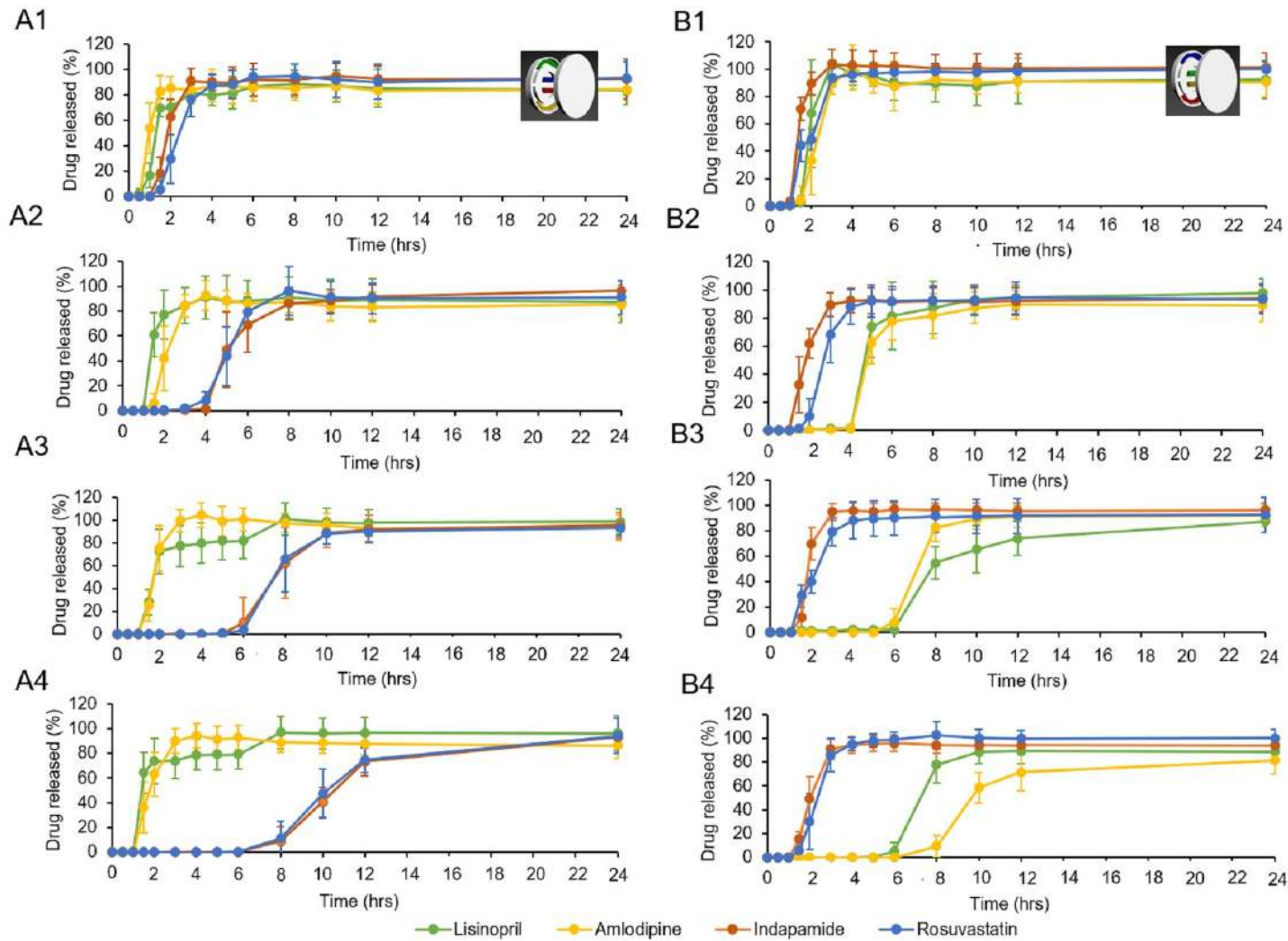


Figure 7 *In vitro* drug release of PVA concentric design capsules with (A1 and B1) 0.6 mm, (A2 and B2) 1.2 mm, (A3 and B3) 1.8 mm and (A4 and B4) 2.4 mm inner wall thickness (n=6).

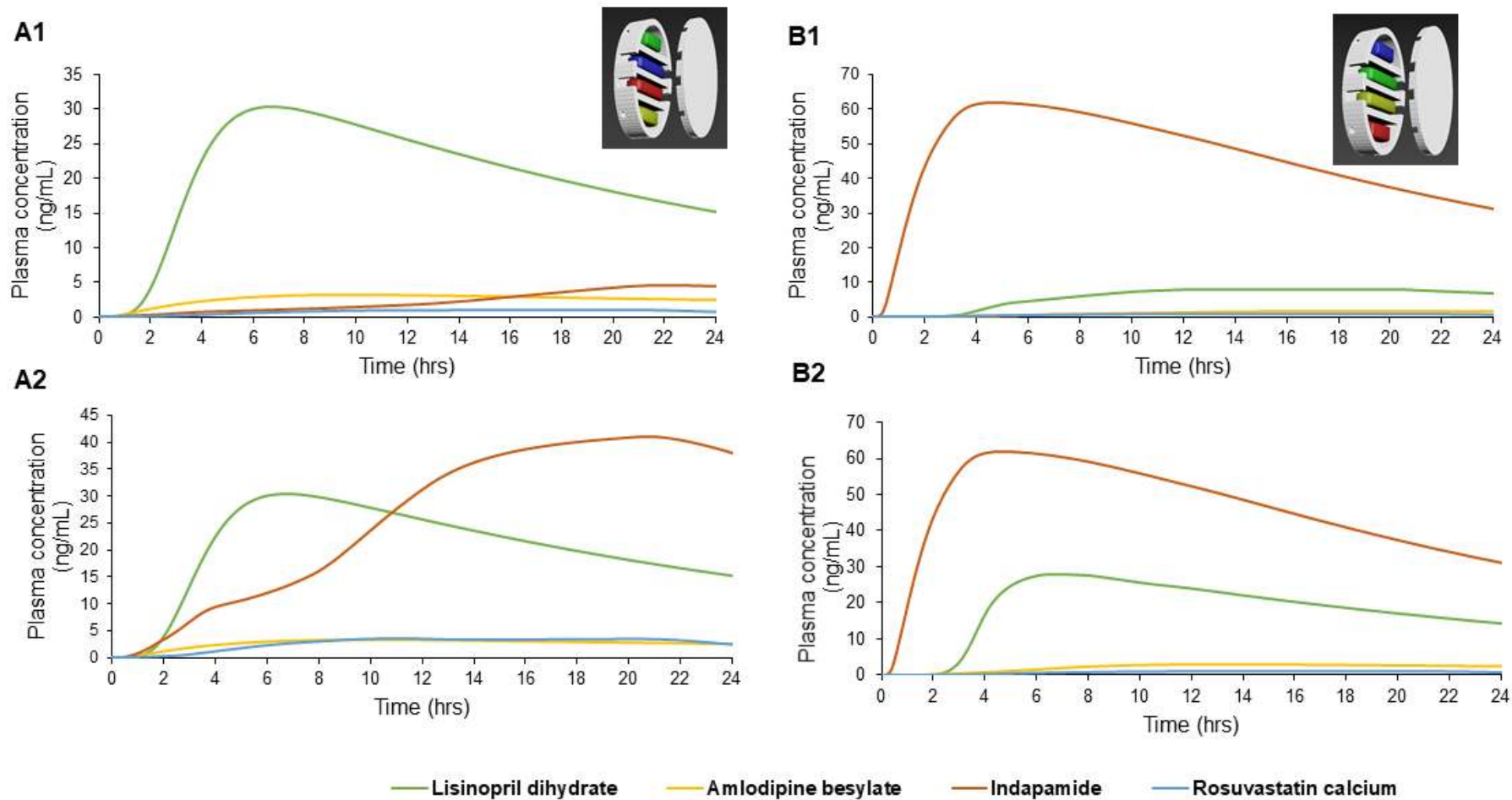


Figure 8 Simulated mean plasma profiles of PLA capsules with 0.25 mm² (A1/B1) and 0.49 mm² (A2/B2) pores PLA capsules, respectively.

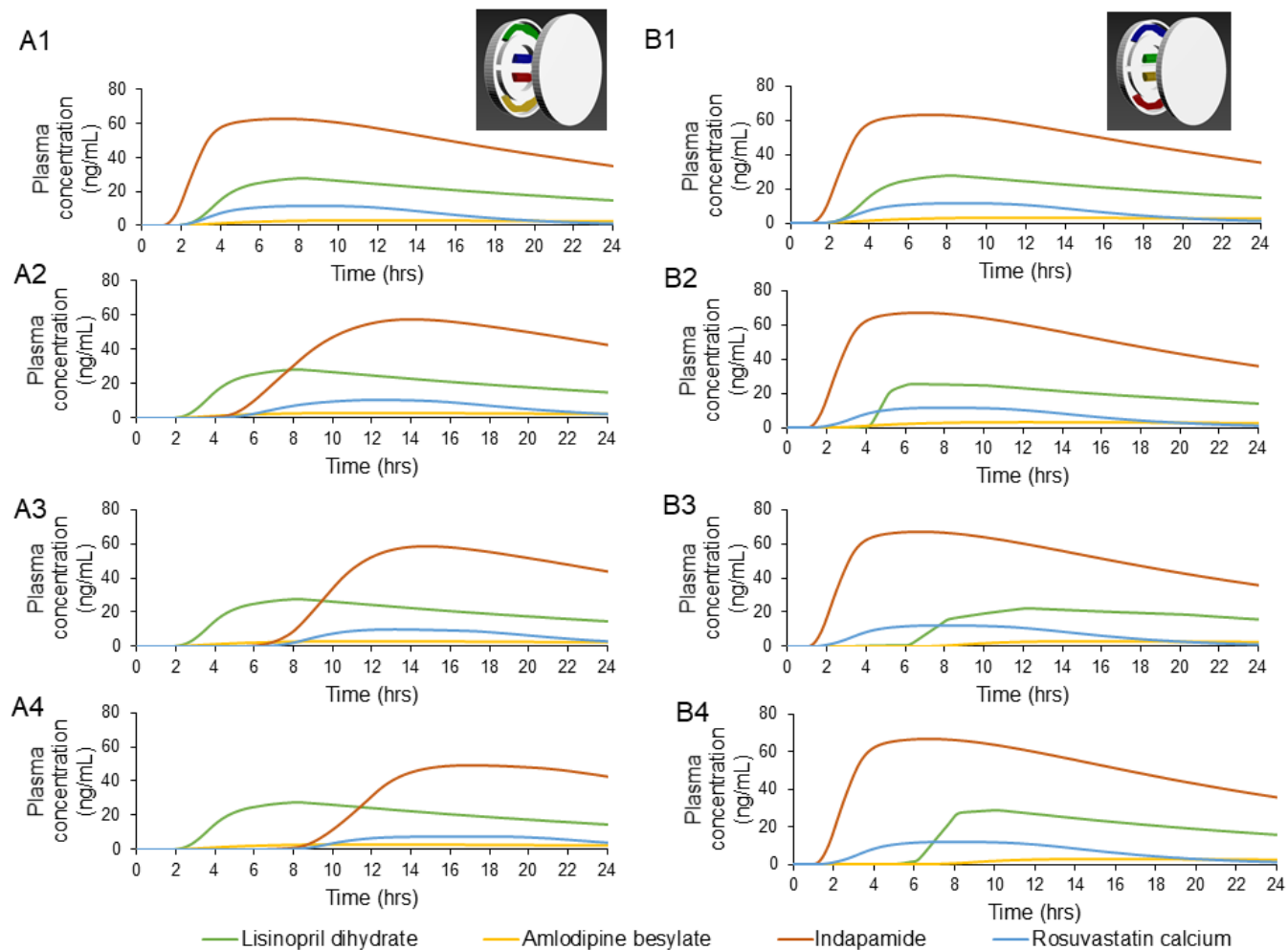


Figure 9 Simulated mean plasma profiles of PVA capsules with 0.6 mm (A1/B1), 1.2 mm (A2/B2), 1.8 mm (A3/B3) and 2.4 mm (A4/B4) wall thickness.

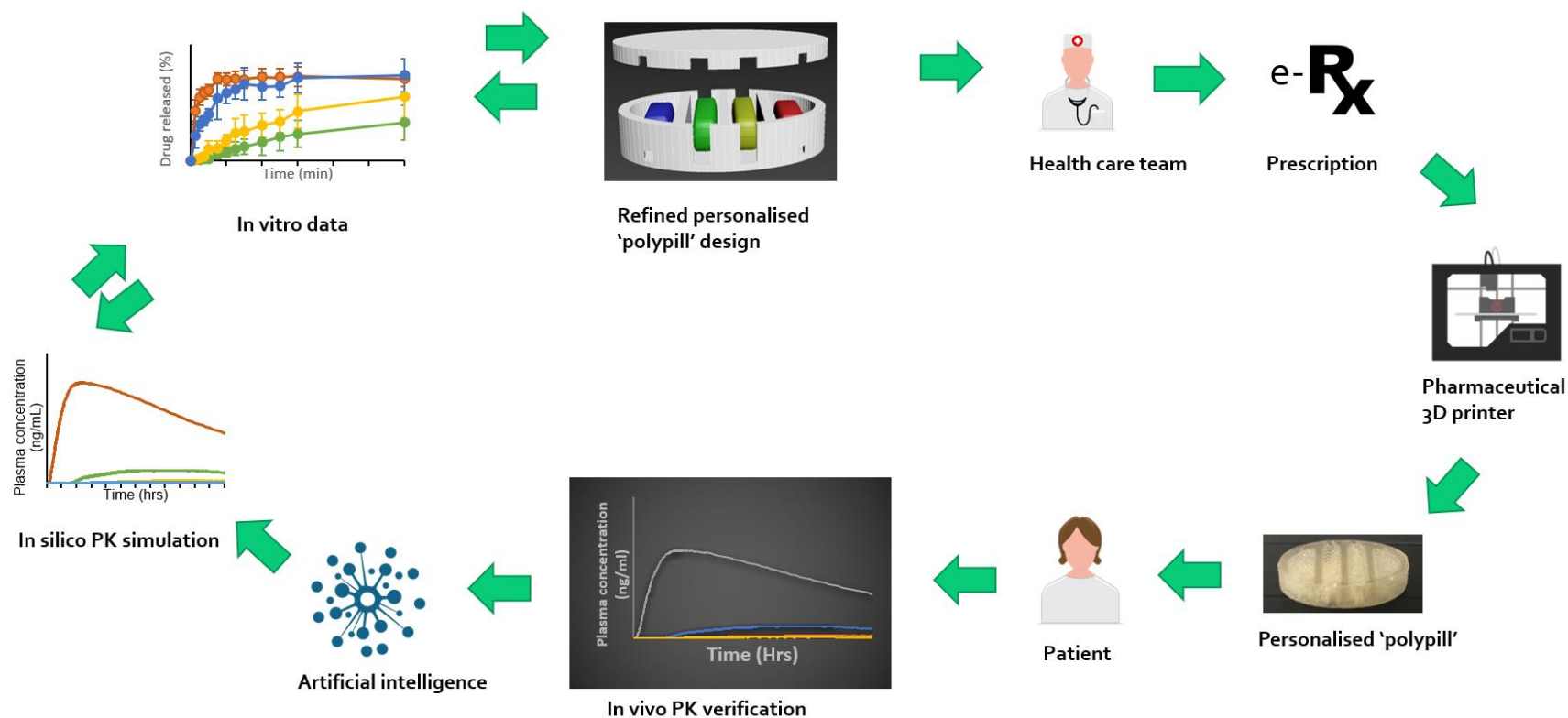


Figure 10 Schematic diagram of future scenario for integrated electronic healthcare system that employ Pharmaceutical 3D printer. The patient’s medical information and genomic specifics will be fed in artificial intelligence system, where target PK simulation will be set. Computer software will help to generate an in vitro plasma profile and a tailored ‘polypill’ design will be built. Healthcare team will approve a corresponding e-prescription and a personalised polypill will be 3D printed and dispensed to the patient. The PK data from patients to improve and maintain target plasma exposure of multiple drugs. The increased number of repeated cycles as well as number participants will improve the accuracy of the system.

Table 1. Composition of hot-filled capsule contents.

Drug-loaded capsule filling	Ingredients (w/w%)						
	Lisinopril dihydrate	Amlodipine besylate	Indapamide	Rosuvastatin calcium	PEG 4000	PEG 400	Lactose monohydrate
Lisinopril dihydrate	10%	-	-	-	10%	30%	50%
Amlodipine besylate	-	5%	-	-	10%	30%	55%
Indapamide	-	-	2.5%	-	10%	30%	57.5%
Rosuvastatin calcium	-	-	-	10%	10%	30%	50%

Table 2. Solubility parameters in MPa^{1/2} and components.

Compound	Solubility parameters			
	δD	δP	δH	HSP
Rosuvastatin	18.7	11.8	10	24.3
Lisinopril	17.1	8.2	9.1	21
Indapamide	21.6	18.9	9.6	30.2
Amlodipine	18	4.3	7.2	19.8
PEG	19.5	13.1	20.3	31